On the Development of Self-Sensing Textile Preforms using Fused Deposition Modelling: A Preliminary Investigation of Process Parameters

C. Keegan[1], B. Khatir[2], M.A.R. Khandoker[2], K. Golovin[2], and A.S. Milani[1]*

[1] Composites Research Network - Okanagan Laboratory, School of Engineering, University of British Columbia, Kelowna, Canada

[2] The Okanagan Polymer Engineering Research and Applications (OPERA) Lab, School of Engineering, University of British Columbia, Kelowna, Canada

* Corresponding author (abbas.milani@ubc.ca)

ABSTRACT

In the pursuit of improved quality and performance of textile-reinforced composites, a great deal of effort in industry has been dedicated to understanding the behaviour of these materials during different stages of manufacturing. In doing so, the direct measurement of the generated defects often represents a challenge, specially for parts with complex shapes, to which Fused Deposition Modelling (FDM) using conductive polymers may prove to be a solution. This study presents the initial results towards developing printed strain sensing elements into textile preforms, through a fractional factorial design of experiments approach to determine the parameters which have the greatest influence over the concurrent mechanical and electrical properties of the 3D printed sensor material, made of a Conductive Polymer Composite of Graphene and PLA. The percent contributions of each printing parameter were calculated with regard to the select performance properties, which included resistance of the sample, peak load, extension at the peak load, toughness, gauge factor and range of constant gauge factor. Finally, three different Multi Attribute Decision Making (MADM) methods and the Entropy weighting were used to determine which parameters would merit highest interest for sensor optimization, by creating an objective ranking of the parameters based on the percent contributions. The overall influence ranking was as follows: 1. Layer Height, 2. Extrusion Multiplier, 3. Nozzle Temperature, 4. Print Speed.

KEYWORDS: *Fused Deposition Modeling, Embedded Sensors, Textile Composites, Multi Attribute Decision Making*

1 INTRODUCTION

Textile composites are an essential type of fiber reinforced polymer composites (FRP). Textile FRP's offer improved impact resistance, shear strength, stiffness (Ekşi and Genel 2017), and formability (Yu et al. 1994a, 1994b) over unidirectional fibers. However, woven fabrics also introduce greater complexity into the prediction and modeling of the reinforcement due to motion of the fibres and out of plane forces (Realff et al. 1997). This additional complexity also makes the validation of these models relatively difficult compared to traditional engineering materials, such as aluminum and steel. Principally, methods for validation rely on optical techniques, such as those used by Ivanov et al. (2009) for the confirmation of a Finite Element simulation. While these systems offer an abundance of information for validation purposes, they are limited by the need for line of sight with the specimen. This limits their use in the validation of forming simulations where areas of interest are likely obscured by forming equipment.

While providing significantly less information than optical methods, strain-based sensors can still provide some of the information necessary for the validation of mathematical models, as is commonly employed for traditional materials. Like with traditional materials, strain sensors can also be used for in-situe monitoring which is often not practical with optical methods. Many of these sensors are constructed from either an electrically conductive material or a fiber optic, which are then woven into the textile of interest (El-Sherif et al. 2000), or bonded to its surface (Cochrane et al. 2007). Strain gauges for traditional materials are usually metal-based, but for textiles the use of Conductive Polymer Composite (CPC) based sensors have drawn greater interest (Cochrane et al. 2010; Mattmann et al. 2008).

The use of CPC's creates several possibilities for the creation of the textile-embedded sensors. Previously mentioned studies (Cochrane et al. 2010; Mattmann et al. 2008) utilized CPC solution masking, or bonding using a silicone film, both being manual processes. Additive manufacturing, specifically Fused Deposition Modeling (FDM), represents a powerful alternative to these manufacturing processes, and CPC based strain sensing structures have already been created using FDM. Leigh et al. (2012), using polycaprolactone (PCL) polymer mixed with Carbon Black (CB), created a series of sensors including a piezoresistive flex sensor and found that the change in resistance of the material under strain was significantly lower than that of conventional sensor materials. McGhee et al. (2018) found that the type of filler can result in larger relative changes in resistance for a given strain. The researchers compared PLA loaded with graphene and CB, and found that graphene resulted in larger relative changes in resistance than the CB. The graphene material was significantly more conductive, 321 Ohm vs 1785 Ohm for a1mm thick sample, meaning that magnitude of change was not as drastic. A commercially available blend of graphene filled PLA was also used to create an embedded strain sensor by Gooding and Fields (2017), and they found that the build orientation of the samples had an impact on the sensor's electrical characteristics. Specifically, there was a large variation between when the load was applied parallel to the layers and when it was applied perpendicular to the layers. In the current literature, this is one of few examinations of the 3D printing parameters' effect on the electrical characteristic of the CPC.

The printing parameters have been examined in a number of different studies with respect to the resultant mechanical properties of the printed part, as summarized by Mohamed et al. (2015). Many of these studies have found that the layer thickness has an influence on mechanical properties of the finished part. Most such studies, however, have focused entirely on the pure polymers, and a few studies on polymer composites (PC) have shown that other process parameters can also have an impact on the resultant mechanical properties. Ning et al. (2017) showed that the nozzle temperature and print speed can, along with layer height, have an impact on the mechanical properties of a fiber reinforced PC. Their study, however, neglected interaction between printing parameters by using a One Factor At a Time (OFAT) approach. Mohamed et al. (2016) showed that these interactions can be statistically significant.

The present article contains preliminary findings from a fractional factorial design of experiments methods on conductive polymer composite specimens manufactured using FDM additive manufacturing. The exploratory study of the FDM parameters was evaluated against both mechanical and electrical properties. The results of these experiments were then evaluated using a series of Multiple Attribute Decision Making (MCDM) methods to objectively determine parameters which merit further investigation as part of our longer-term research program on the development of self-sensing textile preforms using fused deposition modeling.

2 EXPERIMENTAL PROCEDURE

2.1 Printed Specimens

All experiments were performed using a CPC called BlackMagic 3D filament from Graphene labs, which is a PLA with graphene filler. The manufacturer reports that this filament has a conductivity of 0.6 ohm-cm as well as providing a number of recommended printing parameters. These recommended parameters were used in the design of a two-level fractional factorial set of experiments. A full factorial set of experiments was not used due to the preliminary nature of these experiments as well as the cost of the material (approximately $1/gram vs. $0.3/ gram for other conductive filaments) and its availability. The factors used are summarized in **Table 1** below.

Table 1 Summary of printing parameters varied for fractional factorial design of experiments

	Nozzle Temperature (°C)	Layer Height (mm)	Print Speed (mm/min)	Extrusion Multiplier
Manufacturer recommended	195-200	0.1-0.2	2000	1.1
High	220	0.3	2200	1.15
Low	190	0.1	1800	1.05

The parameters were chosen both in accordance with the literature, such as in Ning et al. (2017) and Mohamed et al. (2016), and for influence on the volume of material extruded (i.e. Extrusion Multiplier). Other process parameters were kept constants between the samples and are summarized below.

Table 2 Constant process parameters

Parameter	**Value**	**Parameter**	**Value**
Nozzle diameter	0.8mm	Extrusion width	0.96mm
Build Platform Temperature	60°C	Filament Diameter	1.75mm
Build Platform Surface	Blue Masking Tape		

The specimens in question were ASTM D638 Type V samples. The rasterization of each layer using Simplify3D software was kept constant, and can be seen in **Figure** 1 with only the number of layers changing with thickness of those layers. The gcode was also generated using Simplify3D.

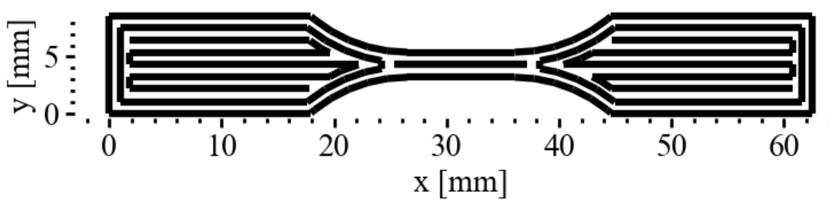

Figure 1: Rasterization of ASTM D638 Type V specimen

The printer used is a modified MakerGear Mk2 printer with a customized heated bed, an E3D V6 hot-end and Titan extruder. **Table** 3 shows the parameters used in the creation of the samples for the half factorial experiments used in this study. The extrusion multiplier was purposely aliased with the interaction of the other parameters to create the half factorial experiment.

Table 3 Specimen printing parameters

Specimen No.	Nozzle Temperature (°C)	Layer Height(mm)	Print Speed (mm/min)	Extrusion Multiplier
1	220	0.3	1800	1.05
2	220	0.3	2200	1.15
3	190	0.1	1800	1.05
4	190	0.3	1800	1.15
5	220	0.1	2200	1.05
6	190	0.3	2200	1.05
7	220	0.1	1800	1.15
8	190	0.1	2200	1.15

2.2 Characterization Tests

As a test of the feasibility of using the FDM process for the creation of a strain sensor on a textile, a sample was created on a sample of dry Twintex woven fabric, which is made of E-glass fibers comingled with polypropylene fibers. The sample was created using the manufacturer recommended settings for temperature and speeds of the CPC. Small loads applied by hand were able to be detected, however when subjected to load using a tensile machine, the sensor failed below 1% strain on the fabric. The results of this test were taken into consideration (i.e. the toughness and the extension at peak load) when selecting the subsequent characterization methods as follows.

The mechanical characterization of the 3D printed polymer was done in accordance with ASTM D638 tensile test using a strain rate of 1mm/minute. The tensile testing machine used was an Instron 5969 universal load frame with a 50kN load cell and double action wedge grips. Said grips were modified by adhering sand paper to the surface of the grips in order to electrically isolate the specimen during testing while trying to eliminate its slipping. Electrical measurements were taken with both a digital multimeter (BK Precision Test Bench 390A), and an Arduino UNO, which was used for datalogging purposes. The Arduino recorded the resistance by way of a voltage divider circuit, as shown in Figure 2, with the resistance being calculated using equation (1).

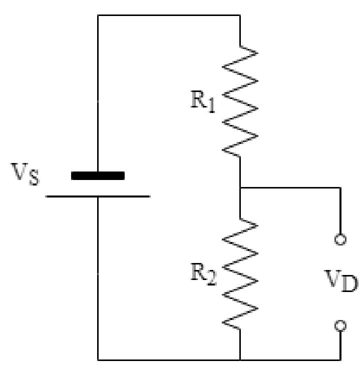

Figure 2: Circuit divider for resistance measurement

$$R_2 = \frac{V_D R_1}{V_S - V_D} \quad (1)$$

R_1 is a known resistance (220Ω), V_S is the voltage provided by the Arduino (3.3V), V_D is the voltage recorded and R_2 is the resistance of interest. A python script was created to record the Arduino output into text files and as well as for post processing. The electrical connection was made by melting the end of a piece of wire onto each end of the samples using an injection molder piston head heated to 220°C. Great care was taken to minimize the amount of heat transferred to the gauge section of the sample.

3 RESULTS AND DISSCUSION

The results of the experiments were analyzed using a combination of the Numpy, Pandas, Scipy and Matplotlib modules in Python. The load and extension data generated by the Instron 5969 load frame were synchronized with the resistance data recorded from the Arduino. The toughness of the specimen was calculated from the area beneath the engineering stress vs. strain curve. The calculation of the gauge factor was done by fitting a linear curve to a plot of the relative change in resistance vs the strain, from which the slope corresponded to the gauge factor. An example of the output can be found in **Figure 3**. This fitted curve was bounded to avoid the influence from the sharp increase in resistance proceeding the failure of the specimen and any initial misalignments of the sample during initial loading. All data, both collected and calculated, can be found in **Table 4**.

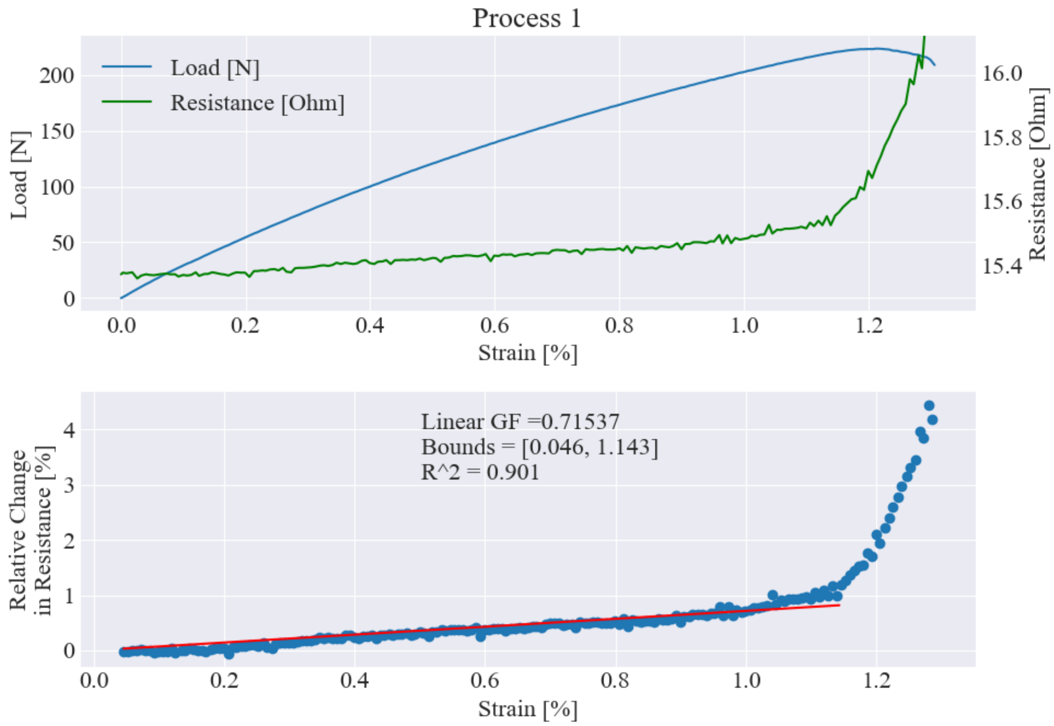

Figure 3: Test data for specimen 1 (corresponding to Table 3 process conditions). The top figure shows the recorded data, the lower figure shows the change in the resistance against the strain. The red line is the fitted curve used for the calculation of the gauge factor.

Table 4 Summary of measured and calculated experimental values. GF = Gauge Factor

Specimen	Resistance (Ω)	Peak Load (N)	Extension at Peak Load (% Strain)	Toughness (kJ/m^3)	GF ($\Delta\Omega/\mathrm{Strain}$)	Width of fit (% Strain)
1	15.8	223.6	1.21	176.6	0.7154	1.10
2	14.8	371.2	2.05	461.0	0.6498	1.97
3	17.4	423.7	3.02	809.6	0.0314	2.08
4	13.4	331.1	4.45	1030.9	0.2930	3.75
5	18.8	359.2	3.45	789.4	-0.4839	2.72
6	13.6	342.9	1.97	407.5	0.2762	1.59
7	19.8	437.1	3.55	977.4	-0.5059	2.91
8	18	439.5	3.49	988.5	0.1486	2.53

Remark: The values reported above for specimens 5 and 7 (per process conditions of Table 3) are found after multiple repeated tests to ensure no structural (outlier) measurement errors. Namely, the original voltage data for specimen (process condition) 7 was clearly erroneous with large jumps in the data, **Figure 4b**, while the data for original specimen 5, **Figure 4a**, exhibited a negative trend upon initial application of the load. None of the other specimen configurations exhibited such outlying trends. The repeated experiments for configurations 5 and 7 exhibited a more pronounced negative trend such as in **Figure 4c** and **4d**. The trends of the repeated tests were similar, but significantly different from the all other tests. As the behaviour of the initial tests was not able to be repeated by any other tests, they were seen as outliers and neglected. The data reported in **Table 4** are based on the repeated tests for configurations 5 and 7. It is believed that such a negative resistance behaviour is related to one or more of the process parameters under scrutiny in these configurations, however the exact cause of this relationship is beyond the scope of the present study.

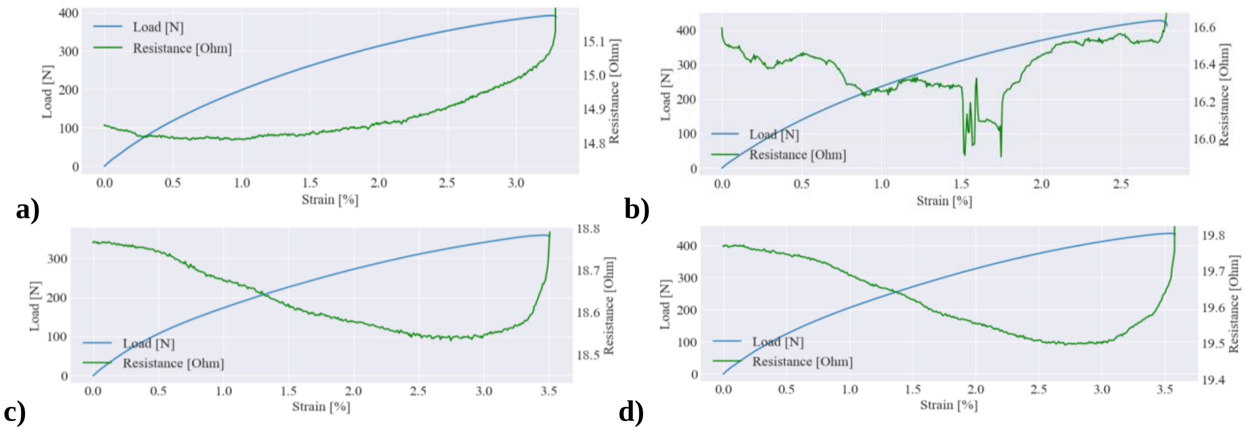

Figure 4: Negative gauge factor behavior of configurations 5 and 7; a) configuration 5 initial data, b) configuration 7 initial data, c) configuration 5 repeated data, d) configuration 7 repeated data

To compare the impact of the different process parameters on the output, the percent contribution was calculated for each process parameter, along with their two-way interactions (**Figure 5**). The higher-level interactions account for the remaining contribution; however, these were not included in **Figure 5** because the 'fractional' factorial nature of the experiment would then result in aliasing of such higher-level interactions.

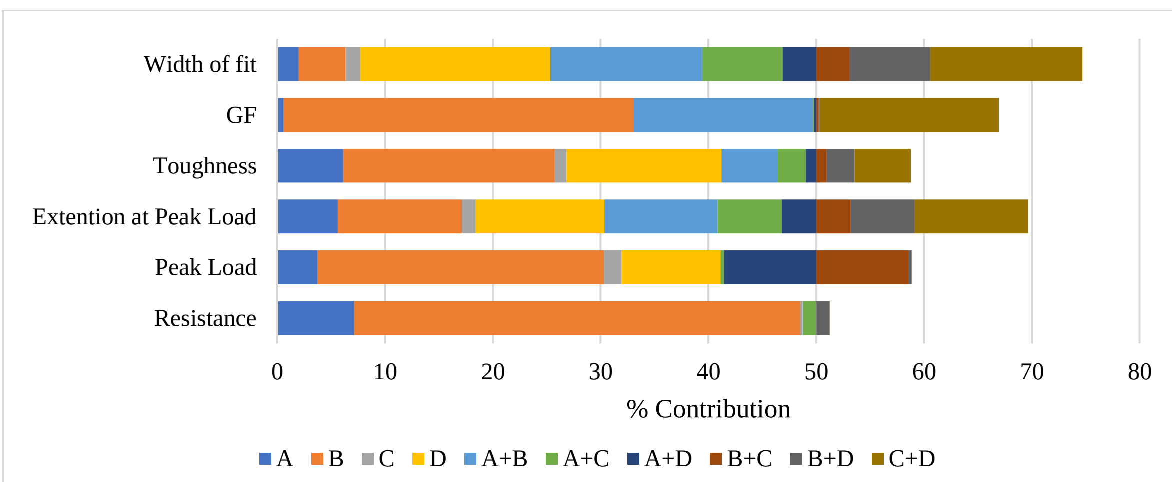

Figure 5: Percent contributions of process parameters and their two-way interactions. A = Nozzle Temperature, B = Layer Height, C = Print Speed, D = Extrusion Multiplier

3.1 Parameter Ranking

To objectively determine the most influential parameters which can be used for further Pareto optimization of the sensor in a future study, a Multi-Attribute Decision-Making (MADM) methodology was employed. Interactions were not included in this section because interactions are not easily controlled directly in practice. The resultant numerical values from Figure 5 are presented in Table 5 as the basis of the MADM problem solving (i.e. as the decision matrix).

Table 5 Percent contributions of the alternatives with respect to the attributes for MADM

		Attributes					
		Resistance	**Peak Load**	**Extension at Peak**	**Toughness**	**GF**	**Width of Fit**
Alternatives	**Nozzle Temperature**	7.11	3.71	5.60	6.13	0.61	2.00
	Layer Height	41.38	26.60	11.52	19.62	32.43	4.32
	Print Speed	0.22	1.65	1.28	1.07	0.01	1.38
	Extrusion Multiplier	0.02	9.16	11.94	14.38	0.01	17.62

For the ranking of the different parameters in Table 5 (i.e. alternatives), a series of compensatory MADM methods were used and the Entropy weighting (Hwang and Yoon 1981) was adapted to determine the relative importance of each attribute (i.e. performance measure of the sensor). The latter was done to make the ranking of the parameters as objective as possible and to create the largest spread of the final scores for ranking. The final values for the relative weights of the values can be found in **Table 6**. The calculated weights clearly prioritized the influence of the electrical performance parameters, which are most important in terms of the measurement properties of a strain-sensing element.

Table 6 Attribute weights for MADM methods determined using the Entropy method

	Attributes					
	Resistance	**Peak Load**	**Extension at Peak**	**Toughness**	**GF**	**Width of Fit**
Weights	0.259	0.117	0.057	0.079	0.356	0.131

These weights were then used in Simple Additive Weighting (SAW), TOPSIS and ELECTRE methods (Yoon and Hwang 1995) to rank the parameters. The summary of rankings of each parameter is shown in **Table 7**, with the parameter meriting the greater investigation being ranked as ‘1’. The average ranking from all three MADM methods was then used as the final ranking scheme.

Table 7 MADM summary of rankings for parameters

Parameters	**SAW**	**TOPSIS**	**ELECTRE**	**Average**
Nozzle Temperature	3	3	2	2.67
Layer Height	1	1	1	1
Print Speed	4	4	4	4
Extrusion Multiplier	2	2	3	2.33

Based on these rankings, the layer height is clearly the best candidate for further optimization of the sensor and the print speed is the least influential. This is in line with other researches that had found that the layer height has the largest impact on the properties of FDM manufactured parts (Mohamed et al. 2016). This held true for almost all parameters including 41% contribution to the change in resistance. The extrusion multiplier and the nozzle temperature are the next ranked parameters, 2nd and 3rd respectively. Based on the values in **Table 5**, the nozzle temperature has a larger impact on the electrical properties (Resistance and Gauge Factor) and the extrusion multiplier has a larger impact on the mechanical properties. This is possibly due to the fact that extrusion multiplier is related to the amount of material extruded, resulting in a probable relation to the load bearing area and porosity of the sample, thus influencing the mechanical properties. The dominant effect of the nozzle temperature on the electrical properties is likely due to either the distribution of the conductive graphene in the extrusions or the bonding between the extrusions. Clearly the print speed has the least impact on the output parameters in this study. The print speed would impact the rate of cooling of the polymer by effecting the amount of time that the hot nozzle is in its proximity. This could affect the degree of crystallization of the polymer, but that does not appear to be the case with the tested blend of graphene and PLA.

4 CONCLUSION AND FUTURE WORK

The study presents initial efforts towards the development of self-sensing textiles using FDM manufacturing. The purpose of the current study was to determine the influence of FDM process parameters on the mechanical and electrical properties of a 3D printed sensor material (based on ASTM D638 Type V specimens) made of filaments of a commercially available polymer blend of PLA and graphene. The percent contribution of each process parameter, as well as their two-way interactions, was calculated. The percent contributions showed that some interactions may be significant when the main parameters are not. This indicates that future work could include all parameters, but that these parameters do not require equal levels of resolution, specially given that interactions are difficult to control in practice for optimization purposes.

A set of compensatory Multi Attribute Decision Making (MADM) methods along with objective weighting was then used to compare the various parameters' overall ranking in terms of their concurrent effects on different mechanical and electrical properties. From these MADM methods, the layer height was found to be overall the most influential factor, followed by the extrusion multiplier, nozzle temperature, and finally the print speed with the least overall influence. The dominating influence of the layer height is consistent with other studies focusing on mechanical properties and different materials. This study also showed that some of the selected parameters can produce a negative gauge factor response, and may be due to the interaction of these parameters and the rasterization of the specimen, although the exact cause of this response requires further investigation. Such future investigations should also include the evaluation of other CPC's, further analysis of the process parameter influence, characterization of the completed textile and development of a methodology for the implementation of FDM manufactured self-sensing textiles.

5 ACKNOWLEDGEMENTS

The authors wish to acknowledge the financial support from the Natural Sciences and Engineering Research Council (NSERC) of Canada. The support from colleagues at the Composites Research Network is also greatly valued.

REFERENCES

Cochrane, C, V Koncar, M Lewandowski, and C Dufour. 2007. "Design and Development of a Flexible Strain Sensor for Textile Structures Based on a Conductive Polymer Composite." *Sensors* 7 (4): 473–92. https://doi.org/10.3390/s7040473.

Cochrane, Cédric, Maryline Lewandowski, and Vladan Koncar. 2010. "A Flexible Strain Sensor Based on a Conductive Polymer Composite for in Situ Measurement of Parachute Canopy Deformation." *Sensors* 10 (9): 8291–8303. https://doi.org/10.3390/s100908291.

Ekşi, S., and K. Genel. 2017. "Comparison of Mechanical Properties of Unidirectional and Woven Carbon, Glass and Aramid Fiber Reinforced Epoxy Composites." *Acta Physica Polonica A* 132 (3): 879–82. https://doi.org/10.12693/APhysPolA.132.879.

El-Sherif, M., K. Fidanboylu, D. El-Sherif, R. Gafsi, J. Yuan, K. Richards, and C. Lee. 2000. "A Novel Fiber Optic System for Measuring the Dynamic Structural Behavior of Parachutes." *Journal of Intelligent Material Systems and Structures* 11 (5): 351–59. https://doi.org/10.1106/JF6U-2FQ9-FQGE-3VXK.

Gooding, Jesse, and Travis Fields. 2017. "3D Printed Strain Gauge Geometry and Orientation for Embedded Sensing." *58th AIAA/ASCE/AHS/ASC Structures, Structural Dynamics, and Materials Conference*, no. February. https://doi.org/10.2514/6.2017-0350.

Hwang, Ching-Lai, and Kwangsun Yoon. 1981. “Methods for Multiple Attribute Decision Making BT - Multiple Attribute Decision Making: Methods and Applications A State-of-the-Art Survey.” In , edited by Ching-Lai Hwang and Kwangsun Yoon, 58–191. Berlin, Heidelberg: Springer Berlin Heidelberg. https://doi.org/10.1007/978-3-642-48318-9_3.

Ivanov, Dmitry, Sergey Ivanov, Stepan Lomov, and Ignaas Verpoest. 2009. “Strain Mapping Analysis of Textile Composites.” *Optics and Lasers in Engineering* 47 (3–4): 360–70. https://doi.org/10.1016/j.optlaseng.2008.05.013.

Leigh, Simon J., Robert J. Bradley, Christopher P. Purssell, Duncan R. Billson, and David A. Hutchins. 2012. “A Simple, Low-Cost Conductive Composite Material for 3D Printing of Electronic Sensors.” Edited by Jeongmin Hong. *PLoS ONE* 7 (11): e49365. https://doi.org/10.1371/journal.pone.0049365.

Mattmann, Corinne, Frank Clemens, and Gerhard Tröster. 2008. “Sensor for Measuring Strain in Textile.” *Sensors* 8 (6): 3719–32. https://doi.org/10.3390/s8063719.

McGhee, J.R., M. Sinclair, D.J. Southee, and K.G.U. Wijayantha. 2018. “Strain Sensing Characteristics of 3D-Printed Conductive Plastics.” *Electronics Letters* 54 (9): 570–72. https://doi.org/10.1049/el.2018.0363.

Mohamed, Omar A., Syed H. Masood, and Jahar L. Bhowmik. 2015. “Optimization of Fused Deposition Modeling Process Parameters: A Review of Current Research and Future Prospects.” *Advances in Manufacturing* 3 (1): 42–53. https://doi.org/10.1007/s40436-014-0097-7.

Mohamed, Omar Ahmed, Syed Hasan Masood, Jahar Lal Bhowmik, Mostafa Nikzad, and Jalal Azadmanjiri. 2016. “Effect of Process Parameters on Dynamic Mechanical Performance of FDM PC/ABS Printed Parts Through Design of Experiment.” *Journal of Materials Engineering and Performance* 25 (7): 2922–35. https://doi.org/10.1007/s11665-016-2157-6.

Ning, Fuda, Weilong Cong, Yingbin Hu, and Hui Wang. 2017. “Additive Manufacturing of Carbon Fiber-Reinforced Plastic Composites Using Fused Deposition Modeling: Effects of Process Parameters on Tensile Properties.” *Journal of Composite Materials* 51 (4): 451–62. https://doi.org/10.1177/0021998316646169.

Realff, M. L., M. C. Boyce, and S. Backer. 1997. “A Micromechanical Model of the Tensile Behavior of Woven Fabric.” *Textile Research Journal* 67 (6): 445–59. https://doi.org/10.1177/004051759706700609.

Yoon, Kwangsun, C L Hwang, and SAGE Research Methods Core. 1995. “Multiple Attribute Decision Making: An Introduction .” Thousand Oaks, CA : Sage Publications .

Yu, Jenny Z., Zhong Cai, and Frank K. Ko. 1994a. “Formability of Textile Preforms for Composite Applications. Part 1: Characterization Experiments.” *Composites Manufacturing* 5 (2): 113–22. https://doi.org/10.1016/0956-7143(94)90062-0.

———. 1994b. “Formability of Textile Preforms for Composite Applications. Part 2: Evaluation of Experiments and Modelling.” *Composites Manufacturing* 5 (2): 113–22. https://doi.org/10.1016/0956-7143(94)90062-0.